On the generation of magnetized collisionless shocks in the large plasma device

D. B. Schaeffer,[1,a)] D. Winske,[2] D. J. Larson,[3] M. M. Cowee,[2] C. G. Constantin,[1] A. S. Bondarenko,[1] S. E. Clark,[1] and C. Niemann[1]
[1]*Department of Physics and Astronomy, University of California-Los Angeles, Los Angeles, California 90095, USA*
[2]*Los Alamos National Laboratory, Los Alamos, New Mexico 87544, USA*
[3]*Lawrence Livermore National Laboratory, Livermore, California 94550, USA*

(Received 29 October 2016; accepted 9 December 2016; published online 22 March 2017)

Collisionless shocks are common phenomena in space and astrophysical systems, and in many cases, the shocks can be modeled as the result of the expansion of a magnetic piston though a magnetized ambient plasma. Only recently, however, have laser facilities and diagnostic capabilities evolved sufficiently to allow the detailed study in the laboratory of the microphysics of piston-driven shocks. We review experiments on collisionless shocks driven by a laser-produced magnetic piston undertaken with the Phoenix laser laboratory and the Large Plasma Device at the University of California, Los Angeles. The experiments span a large parameter space in laser energy, background magnetic field, and ambient plasma properties that allow us to probe the physics of piston-ambient energy coupling, the launching of magnetosonic solitons, and the formation of subcritical shocks. The results indicate that piston-driven magnetized collisionless shocks in the laboratory can be characterized with a small set of dimensionless formation parameters that place the formation process in an organized and predictive framework. *Published by AIP Publishing.*
[http://dx.doi.org/10.1063/1.4978882]

I. INTRODUCTION

Collisionless shocks were first discovered around Earth in the early 1960s and have since been observed around many of the planets of the solar system, in artificial plasma releases in the magnetosphere, in coronal mass ejections, and at the heliopause.[1–5] These shocks convert incoming upstream ram pressure to downstream thermal pressure over length scales much shorter than the classical mean free path. In planetary systems such as the Earth's magnetosphere, bow shocks occupy a wide range of magnetic field geometries (from quasi-perpendicular to quasi-parallel) and Mach numbers, including the class of low-Mach number ($M \lesssim 3$), subcritical collisionless shocks that generate entropy in the shock layer through resistive dissipation.

While the study of collisionless shocks would eventually become dominated by spacecraft observations by the 1980s, collisionless shocks were at first primarily investigated through laboratory experiments.[6–8] These early efforts were largely carried out on pinches and sought to generate collisionless shocks by driving a magnetic piston through an ambient plasma. The experiments were successful in generating collisionless shocks up to $M \sim 6$; however, the main results were often not directly relevant to space shocks since they were generally concerned with shock heating (in particular electron heating) and the experimental setups were confined to strictly perpendicular magnetic geometries.[9] As spacecraft measurements became more prevalent, laboratory experiments ceased altogether.

Decades later, the realization that both spacecraft and numerical simulations were limited in their ability to fully capture shock physics renewed interest in the laboratory study of collisionless shocks. Several authors[10–12] collectively argued that shocks of cosmic relevance could be generated in the laboratory using high-energy lasers, which afforded several advantages over pinches. Lasers could not only impart higher energies to the shocked plasma to drive higher Mach numbers or larger system sizes but could also allow flexibility in magnetic field geometry, since the direction of piston propagation could be made at arbitrary angles relative to the background magnetic field.

Over the past decade, the proliferation of high-energy lasers has allowed experimentalists to begin realizing the goal of generating and diagnosing a wide variety of collisionless shocks relevant to space and astrophysics. These efforts have focused primarily on laser-driven magnetic pistons[13–16] and laser-driven counter-streaming setups[17] and have resulted in the successful generation of a laser-driven subcritical magnetized shock,[18] the successful generation of laser-driven electrostatic shocks,[19,20] the first attempts at Weibel-mediated shocks,[21] and new pinch-based experiments using lasers.[22]

In this paper, we review recent efforts to generate collisionless shocks through a laser-driven magnetic piston in the LArge Plasma Device (LAPD) at the University of California, Los Angeles (UCLA). In particular, we focus on experiments in the subcritical regime in a quasi-perpendicular geometry, and we build on the work of Drake[23] and Zakharov[24] to describe a set of shock formation criteria relevant to laser-driven magnetic pistons. A brief overview of these previous experiments is given in Sec. II,

[a)]Electronic mail: dschaeffer@physics.ucla.edu

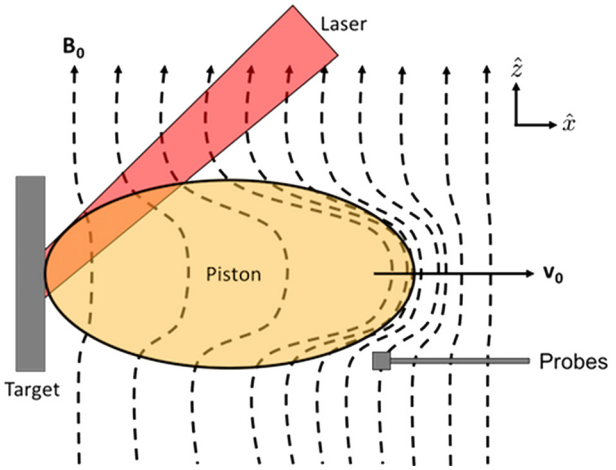

FIG. 1. Schematic of LAPD experiments. In a fluid picture, the background magnetic field is pulled by the expanding piston (laser-ablated) ions to conserve magnetic flux, resulting in a magnetic cavity and leading magnetic compression. At the same time, the moving magnetic compression pulls on the ambient ions, accelerating them to speeds comparable to the piston. The magnetic field and density profiles were probed with magnetic flux ("bdot"), emissive, and Langmuir probes.

and the formation criteria and their application to LAPD experiments are discussed in Sec. III.

II. REVIEW OF SHOCK EXPERIMENTS ON THE LAPD

In this section, we briefly review the results from collisionless shock experiments on the LAPD at UCLA. A general diagram of the setup for the experiments is shown in Fig. 1. The LAPD[25] is a cylindrical vacuum vessel (20 m long × 1 m diameter) that can generate a steady-state (∼15 ms), magnetized ambient plasma at high-repetition (up to 1 Hz). The machine is well-suited for shock experiments because of its variable background magnetic field (200–1500 G), variable ambient plasma (He^{+1}, He^{+1}), variable ambient density (10^{12}–10^{13} cm^{-3}), and large volume (>50 cm across the plasma column). The LAPD was coupled with high-energy (<300 J) lasers from the Phoenix laser laboratory,[26] which irradiated a plastic or graphite target embedded in the LAPD ambient plasma. The ablated piston plasma then expanded across the background field and through the ambient plasma in a quasi-perpendicular magnetic geometry. The piston speed could be adjusted by tuning the laser intensity. A summary of LAPD shock experiments is given in Table I, and magnetic profiles from a subset of these experiments are shown in Fig. 2.

The first sets of experiments were undertaken at low laser energies (<25 J) and at low ambient plasma densities ($\sim 5 \times 10^{12}$ cm^{-3}, see Exp. 1–3 in Table I and Fig. 2(a)). Building on earlier work,[27] high-repetition experiments[28] with a 1 J laser successfully created large-diameter (∼30 cm) diamagnetic cavities and expanding magnetic compressions. However, these magnetic pulses propagated sub-Alfvénically ($M_A < 1$) and the background magnetic field was not fully expelled in the cavity. Follow-on experiments[14] were conducted at higher laser energies (∼25 J), which allowed the piston plasma to expand super-Alfvénically ($M_A \sim 1 - 3$). As a result, the background field was fully expelled in the cavity, the magnetic field was significantly compressed ($B/B_0 \sim 1.5$), and a propagating magnetosonic soliton was observed, though no shock formed. Nonetheless, these experiments demonstrated the viability of a magnetic piston on the LAPD.

Upgrades were then undertaken on both the LAPD and Phoenix laser facility, which allowed higher ambient densities ($\sim 2 \times 10^{13}$ cm^{-3}) and laser energies (∼100 J). Experiments[15] at these conditions revealed new features, including magnetic compression factors as large as the Mach number, which is expected for low-Mach number shocks (see Exp. 4 and 5 in Table I and Fig. 2(b)). Unlike the low-energy experiments, the magnetic cavities created by the piston ions were smaller with an ambient plasma than without, suggesting that some energy from the piston ions was being transferred into accelerating the ambient plasma. However, no steepening of the magnetic field was observed at the leading edge of the magnetic compression. As a result, these large-amplitude magnetic pulses were identified as *pre-shocks* and indicated that energy from the piston was being coupled into the ambient plasma, but the system size was too

TABLE I. Summary of representative experiments undertaken on the LAPD. Listed are the laser energy E_0 and intensity I_0 on target, composition of the piston (laser-ablated) and ambient plasmas, initial piston expansion speed v_0, background magnetic field B_0, ambient density n_a, and experimental system size D_0. Also shown are the dimensionless formation criteria discussed in Sec. III.

	Exp. 1	Exp. 2	Exp. 3	Exp. 4	Exp. 5	Exp. 6	Exp. 7
E_0 (J)	1	20	20	90	100	190	180
I_0 (W/cm^2)	0.6×10^{11}	4.7×10^{11}	4.7×10^{11}	1.4×10^{11}	1.5×10^{11}	1.2×10^{12}	4.6×10^{12}
Piston ions	C^{+4}	C^{+4}	C^{+4}	C^{+4}	C^{+4}	C^{+4}	C^{+4}
Ambient ions	He^{+1}	H^{+1}	He^{+1}	H^{+1}	He^{+1}	H^{+1}	C^{+4}
v_0 (km/s)	150	410	380	260	220	400	54
B_0 (G)	600	275	275	200	200	300	400
n_a (cm^{-3})	2×10^{12}	2×10^{12}	5×10^{12}	5×10^{12}	5×10^{12}	1.2×10^{13}	5.0×10^{13}
D_0 (cm)	40	35	35	35	35	45	20
M_A	0.3	1.0	2.8	1.3	2.3	2.1	1.5
λ_{ii}/D_0	>100	>100	>100	>100	>100	>100	0.1
ρ_p/R_m	0.8	1.6	3.2	1.0	1.3	1.4	0.6
ρ_a/R_*	0.8	0.8	3.9	0.5	1.6	0.7	0.6
ρ_i/D_0	0.3	1.3	1.6	1.2	1.3	0.9	0.2

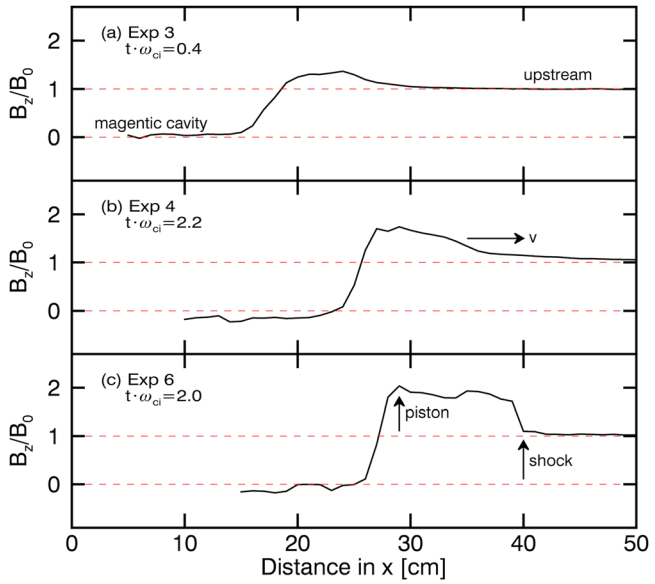

FIG. 2. Profiles of B_z normalized to the background field B_0 for (a) Exp. 3, (b) Exp. 4, and (c) Exp. 6 in Table I. The profiles are shown at peak magnetic compression (at a time given in units of the upstream ambient ion gyrofrequency ω_{ci}) and were measured by magnetic flux probes over multiple laser shots. The target is at $x = 0$, and the magnetic pulses move to the right. (a) Despite having a fully expelled magnetic cavity and being $M_A \sim 3$, only a weak ($B_z/B_0 \sim 1.4$) magnetic pulse was observed in a He^{+1} plasma. (b) Increases in ambient density and laser energy resulted in a stronger ($B_z/B_0 \sim 1.8$) magnetic compression, but no steepening was observed at the leading edge. (c) Additional laser upgrades resulted in a $M_A \sim$ 2-2.5 collisionless shock with a magnetic compression of $B_z/B_0 \sim$ 2-2.5 that was observed separating from the magnetic piston.

small at those conditions for a shock to form (generally limited by the size of the ambient plasma).

Additional upgrades to the laser system resulted in available laser energies up to 200 J. The extra energy not only resulted in more energetic pistons, but it also allowed more flexibility in the design of the piston. By tuning the laser intensity, more piston ions could be ablated (allowing more energy coupling) while keeping the piston ion speeds super-Alfvénic. Consequently, experiments[15,29] at these parameters were successful for the first time in generating a laser-driven, low-Mach number collisionless shock[18] (see Exp. 6 in Table I and Fig. 2(c)). Similar to the pre-shock case, large magnetic compressions commensurate with the Mach number were observed. In addition, the leading edge of the magnetic compression steepened and began separating from the piston, indicative of a collisionless shock. It is worth noting here that experiments[30] at similar laser energies were undertaken at the Trident laser facility[31] (see Exp. 7 in Table I). The primary difference was that both the piston and ambient plasma were composed of carbon ions, and only a pre-shock was observed.

III. DIMENSIONLESS CRITERIA FOR SHOCK FORMATION

In the experiments reviewed in Sec. II, the fundamental experimental parameters are the background magnetic field B_0, ambient ion density n_0, piston velocity v_0, number of ablation piston ions N_0, piston ion ionization Z_p and mass m_p, ambient ion ionization Z_a and mass m_a, and system size D_0. Utilizing those experiments, we identify five criteria that incorporate these parameters and that must be simultaneously satisfied to allow shock formation through a laser-driven magnetic piston. These criteria expand upon those outlined by Drake[23] and in some cases are modifications to those discussed by Zakharov.[24] The criteria are:

1. $M_A > 1$
2. $\lambda_{ii}/D_0 > 1$
3. $\rho_p/R_m \leq \sqrt{2}$
4. $\rho_a/R_* \leq 1$
5. $\rho_i/D_0 < 1$

The first two criteria are evident for collisionless shocks. First, the accelerated ambient ions must be super-Alfvénic

$$M_A = v_0/v_A \geq 1, \tag{1}$$

where v_A is the Alfén speed in the unperturbed (upstream) ambient plasma. Here, we have assumed that the accelerated ambient speed is equivalent to the piston expansion speed v_0, which is generally a good approximation when the two are well coupled.[32] In practice, then, this criterion requires a super-Alfvénic piston. Second, the accelerated ambient ions must be collisionless relative to the stationary ambient ions

$$\lambda_{ii}/D_0 > 1, \tag{2}$$

where λ_{ii} is the ambient ion-ion collisional mean free path evaluated for accelerated ambient ions with speed v_0. Note that only the ambient ion-ion interaction must be collisionless; it is possible for the piston-ambient ion interaction to be collisional (though it generally is not) or for the upstream ambient ions to be collisional.

The third and fourth criteria specifically regard a laser-driven magnetic piston. The ratio of the gyroradius of the piston ions to the equal mass radius must satisfy

$$\rho_p/R_m \leq \sqrt{2}. \tag{3}$$

Here, $\rho_p = v_0/\omega_{ci,p}$ is the directed piston ion gyroradius with gyrofrequency $\omega_{ci,p} = Z_p eB_0/m_p c$, and $R_m = (3N_0 m_p/4\pi m_a n_a)^{1/3}$ is the equal mass radius and is the distance required for the piston ions to sweep out an equivalent mass of ambient ions. The condition of Eq. (3) says that the piston ions must be sufficiently magnetized and is related to how energy and momentum are transferred between the piston and ambient ions. Hewett *et al.*[32] demonstrated through hybrid simulations and test particle calculations that as the piston ions are deflected by the background magnetic field, they generate a transverse electric field that allows the momentum and energy of the piston ions to be transferred to the ambient ions in a process known as Larmor coupling. If the piston ion gyroradius is larger than R_m, though, the piston ions stream out past the expected stopping distance and fail to couple effectively, instead generating a weak magnetic pulse. Simulations[33] have indicated that the cutoff value should be $\sqrt{2}$ and have shown the validity of this condition for characterizing shock formation.

The fourth criterion is similar:

$$\rho_a/R_* \leq 1. \tag{4}$$

Here, $\rho_a = v_0/\omega_{ci,a}$ is the directed gyroradius of ambient ions that have been accelerated to the piston speed and $R_* = (3N_0Z_p/4\pi Z_a n_a)^{1/3}$ is the equal charge radius,[34] which is the distance over which the charged piston ions have overrun an equal charge density of ambient ions. R_* can be thought of as the distance over which the ambient ions become effectively magnetized, since it is the characteristic distance at which Larmor coupling to the ambient ions effectively ends (since the charge densities are then equivalent). Eq. (4) then is just the consequence of requiring that the final accelerated ambient ion speed acquired during the coupling phase is larger or equal to the piston speed. Note that

$$\left(\frac{R_*}{R_m}\right)^3 = \left(\frac{Z_p}{Z_a}\frac{m_a}{m_p}\right) = \frac{\rho_a}{\rho_p}. \tag{5}$$

For convenience, we define the degree of magnetization of the ambient ions relative to the piston ions as a magnetization factor, M

$$M = \left(\frac{Z_a}{Z_p}\frac{m_p}{m_a}\right). \tag{6}$$

Consequently, $R_* = M^{-1/3}R_m$ and the fourth criterion (Eq. (4)) can be written

$$\rho_a/R_* = \frac{1}{M^{2/3}}\frac{\rho_p}{R_m} \leq 1. \tag{7}$$

Evidently, for $M > 2^{3/4} \approx 1.68$, Eq. (7) is satisfied whenever Eq. (3) is satisfied. For smaller values of M, Eq. (7) replaces the third condition (Eq. (3)) with the more restrictive condition

$$\rho_p/R_m \leq M^{2/3}. \tag{8}$$

As an example, consider a typical LAPD experiment in which C^{+4} piston ions expand into a H^+ or He^+ ambient plasma. For a H plasma, $M = 3$ and Eq. (4) will be satisfied whenever Eq. (3) is satisfied. However, with a He ambient plasma, $M = 0.75$ and $M^{-2/3} \approx 1.21$. As a result, Eq. (4) is satisfied only when $\rho_p/R_m < 0.83$ (Eq. (8)). In other words, in the case of He ions that are less magnetized than H ions, to form a shock the piston ions have to be even more magnetized (i.e., smaller gyroradii relative to the equal mass radius) during the expansion so that they can magnetically couple to the ambient ions before the piston ions stop at a distance $r \sim R_m$.

We note that variations of the magnetization criteria (i.e., Eqs. (3) and (4)) have been found in other works. In Ref. 35, Golubev *et al.* adopt the condition $\rho_a/R_* \leq 1$ but assume $\rho_a = \rho_p$. In contrast, Bashurin *et al.* in Ref. 34 find the condition $R_*^2/(\rho_a\rho_p) \geq 2.8$. Additionally, recent work[36] by Larson *et al.* in the strong coupling limit suggests the alternative conditions $\rho_a/R_* \leq 1/2$ and $\rho_p/R_* \leq 1$.

Finally, both the piston and ambient ion gyroradii ρ_i must be smaller than the system size

$$\rho_i/D_0 < 1. \tag{9}$$

For very small systems, this more stringent condition replaces Eq. (3) and/or Eq. (4).

From the basic experimental parameters, generally the background field and ion masses (through the target material and ambient gas fill) are easiest to vary. Conversely, it is generally difficult to significantly vary the ambient ion density, ion charge states, and system size. Both the piston velocity and number of piston ions can be varied through laser intensity I_0 ($N_0 \propto I_0^{5/9}$ and $v_0 \propto I_0^{2/9}$).[37] While the number of piston ions is more sensitive to laser intensity, it is generally easier to measure the piston velocity. Consequently, in the following we consider the background field and piston velocity to be the primary experimental variables.

Fig. 3 shows the formation criteria as a function of B_0 and v_0 for fixed n_a, N_0, and D_0. The first two panels are under current LAPD and laser conditions for a C^{+4} piston plasma expanding into a H^{+1} ($M = 3$) and He^{+1} ($M = 0.75$) ambient plasma. In He, the available parameter space for generating

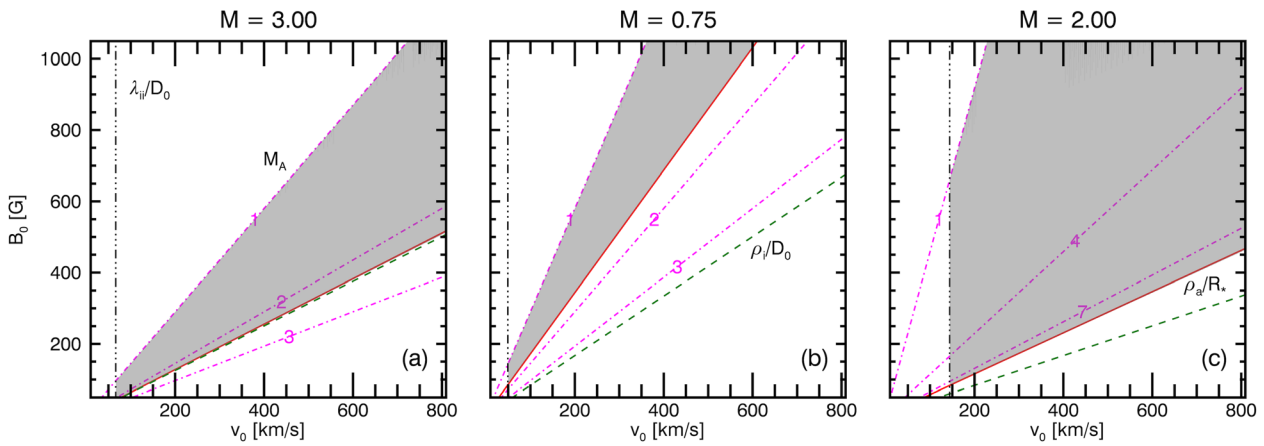

FIG. 3. Shock formation criteria as functions of background magnetic field B_0 and piston speed v_0 for fixed ambient density n_a, number of ablated ions N_0, and system size D_0. The shaded areas are the regions where all criteria are satisfied. The magnetization M is above each panel, where $M = 3$ represents C^{+4} expanding into H^{+1}, $M = 0.75$ represents C^{+4} expanding into He^{+1}, and $M = 2$ represents C^{+6} expanding into H^{+1}. Panels (a) and (b) are typical for the LAPD and a 250 J laser, with $n_a = 10^{13}$ cm^{-3}, $N_0 = 1.5 \times 10^{17}$, and $D_0 = 50$ cm. Panel (c) corresponds to planned upgrades to the LAPD and Phoenix laser facility, with $n_a = 10^{14}$ cm^{-3}, $N_0 = 6.0 \times 10^{17}$, and $D_0 = 50$ cm.

collisionless shocks is limited to a small space of low Mach numbers. While it would be possible to generate a $M_A \sim 1.5$ shock, it would be difficult to distinguish the shock from magnetic compressions of order 50% that can be generated by the diamagnetic current. The available parameter space is considerably better in H, but even then shocks would generally still be limited to subcritical Mach numbers $M_A < 2.5$. Fig. 3(c) shows the formation criteria for planned upgrades to the LAPD and Phoenix laser facility. An increase in ambient density relaxes the magnetization and system size constraints, allowing supercritical shocks ($M_A > 3$) to be generated. Simultaneously, upgraded laser intensities of $\sim 10^{13}$ W/cm^2 increase the number of ablated ions and piston charge state, expanding the parameter space to $M_A \gtrsim 7$ shocks.

The formation criteria can also be compared against the experiments discussed in Sec. II. Fig. 4 shows where LAPD experiments lie in a parameter space defined by the magnetization criteria (Eqs. (3) and (4)). The experiments are organized by the ambient plasma used (indicated by different shapes) and whether they satisfied the non-magnetization formation criteria (indicated by different colors). The lower-left region of the parameter space is where all formation criteria are fulfilled and is where collisionless shocks are expected to form (the "shock region").

Generally, experiments where collisionless shocks were observed agree well with the location of those experiments in the magnetization parameter space. Their location near the ρ_p/R_m cutoff is also consistent with the generally marginal conditions in which the shocks formed (see, for example, Fig. 3(a)). The location of several experiments within the shock region, but that were larger than the system size, is also consistent with the observation of pre-shocks, since these would be expected to develop into shocks given enough space and time. Fig. 4 also reinforces the difficulty of driving collisionless shocks in low-magnetization conditions as seen in Fig. 3(b). Experiments with a He ambient plasma at a variety of laser energies, ambient densities, and piston speeds were almost exclusively confined to outside of the shock region (most of these fall outside the bounds of Fig. 4). Conversely, experiments with a carbon ambient plasma, like those[30] undertaken on the Trident laser facility, show potential for driving shocks if the piston speed can be kept high enough to keep the ambient-ion-ion interaction collisionless.

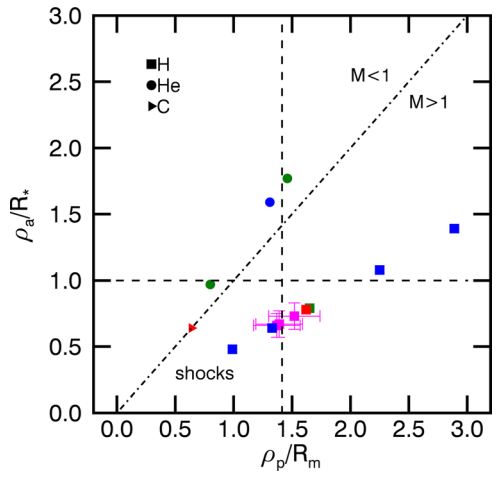

FIG. 4. Magnetization parameter space with LAPD experiments. The dashed lines indicate the conditions that the magnetization criteria need to satisfy (i.e., $\rho_p/R_m \leq \sqrt{2}$ and $\rho_d/R_* \leq 1$), and the region where collisionless shocks are expected to form is labeled. The dotted line separates the lower region where the ambient ions are more magnetized ($M > 1$) from the upper region where the piston ions are more magnetized ($M < 1$). The experimental points are categorized by ambient plasma (shape) and are shown with error bars. The experiments are also colored according to how many formation criteria were satisfied: purple if a shock was observed; green if all non-magnetization formation criteria were satisfied; blue if the experiment was larger than the system size; and red if the experiment was sub-Alfvénic or collisional.

IV. CONCLUSION

Laser-driven collisionless shocks are an important new class of laboratory astrophysics experiments. Here, we have focused on shock experiments on the LAPD that utilize a laser-driven magnetic piston and that encompass a wide range of laser, plasma, and magnetic field parameters. Correspondingly, the results span a range of shock-related features, including large-diameter, sub-Alfvénic magnetic cavities; super-Alfvénic magnetosonic solitons; low-Mach number pre-shocks; and subcritical collisionless shocks. These outcomes are consistent with how well the experiments satisfy several formation criteria. In particular, experiments in which collisionless shocks were observed agree well with the conditions that the piston and ambient plasmas be sufficiently magnetized, while simultaneously being super-Alfvénic, collisionless, and small enough to fit within the experimental volume.

These criteria should also extend to supercritical ($M_A \gtrsim 3$) collisionless shocks, where ion reflection at the shock front is important. Experiments at multi-kJ laser facilities that utilize significantly higher magnetic fields and ambient densities, and which can more easily drive high-Mach number shocks, should be able to test this assumption. Future upgrades to the LAPD and Phoenix laser facility will also allow experiments to drive higher-Mach number shocks up to $M_A \approx 7$. Experiments will continue on the LAPD to study subcritical shock formation relevant to space shocks, while new experiments have begun to investigate quasi-parallel magnetic geometries uniquely possible on the LAPD.

ACKNOWLEDGMENTS

This work was supported by DTRA under Contract No. HDTRA1-12-1-0024, DOE under Contract Nos. DE-SC0006538:0003 and DE-NA0001995, and NSF Award No. 1414591.

[1]E. J. Smith, L. Davis, D. E. Jones, P. J. Coleman, D. S. Colburn, P. Dyal, and C. P. Sonett, Science **188**, 451 (1975).
[2]E. J. Smith, L. Davis, D. E. Jones, P. J. Coleman, D. S. Colburn, P. Dyal, and C. P. Sonett, Science **207**, 407 (1980).
[3]A. Valenzuela, G. Haerendel, H. Foppl, F. Melzner, H. Neuss, E. Rieger, J. Stocker, O. Bauer, H. Hofner, and J. Loidl, Nature **320**, 700 (1986).
[4]L. F. Burlaga, N. F. Ness, M. H. Acuna, R. P. Lepping, J. E. P. Connerney, and J. D. Richardson, Nature **454**, 75 (2008).

[5]A. Balogh and R. A. Treumann, *Physics of Collisionless Shocks*, ISSI Scientific Report Series Vol. 12 (Springer, 2013).
[6]J. W. M. Paul, L. S. Holmes, M. J. Parkinson, and J. Sheffield, Nature **208**, 133 (1965).
[7]A. W. DeSilva and J. A. Stamper, Phys. Rev. Lett. **19**, 1027 (1967).
[8]J. A. Stamper and A. DeSilva, Phys. Fluids **12**, 1435 (1969).
[9]C. F. Kennel, J. P. Edmiston, and T. Hada, "A quarter century of collisionless shock research," in *Collisionless Shocks in the Heliosphere: A Tutorial Review* (American Geophysical Union, Washington, DC, 1985), pp. 1–36.
[10]R. P. Drake, J. Geophys. Res. **104**, 14505, doi:10.1029/98JA02829 (1999).
[11]D. Ryutov, R. P. Drake, J. Kane, E. Liang, B. A. Remington, and W. M. Wood-Vasey, Astrophys. J. **518**, 821 (1999).
[12]B. A. Remington, D. Arnett, R. Paul, Drake, and H. Takabe, Science **284**, 1488 (1999).
[13]C. Constantin, W. Gekelman, P. Pribyl, E. Everson, D. Schaeffer, N. Kugland, R. Presura, S. Neff, C. Plechaty, S. Vincena, A. Collette, S. Tripathi, M. Muniz, and C. Niemann, Astrophys. Space Sci. **322**, 155 (2009).
[14]C. Niemann, W. Gekelman, C. G. Constantin, E. T. Everson, D. B. Schaeffer, S. E. Clark, D. Winske, A. B. Zylstra, P. Pribyl, S. K. P. Tripathi, D. Larson, S. H. Glenzer, and A. S. Bondarenko, Phys. Plasmas **20**, 012108 (2013).
[15]D. B. Schaeffer, E. T. Everson, A. S. Bondarenko, S. E. Clark, C. G. Constantin, D. Winske, W. Gekelman, and C. Niemann, Phys. Plasmas **22**, 113101 (2015).
[16]I. F. Shaikhislamov, Y. P. Zakharov, V. G. Posukh, A. V. Melekhov, E. L. Boyarintsev, A. G. Ponomarenko, and V. A. Terekhin, Plasma Phys. Rep. **41**, 399 (2015).
[17]H. Park, D. Ryutov, J. Ross, N. Kugland, S. Glenzer, C. Plechaty, S. Pollaine, B. Remington, A. Spitkovsky, L. Gargate, G. Gregori, A. Bell, C. Murphy, Y. Sakawa, Y. Kuramitsu, T. Morita, H. Takabe, D. Froula, G. Fiksel, F. Miniati, M. Koenig, A. Ravasio, A. Pelka, E. Liang, N. Woolsey, C. Kuranz, R. Drake, and M. Grosskopf, High Energy Density Phys. **8**, 38 (2012).
[18]C. Niemann, W. Gekelman, C. G. Constantin, E. T. Everson, D. B. Schaeffer, A. S. Bondarenko, S. E. Clark, D. Winske, S. Vincena, B. Van Compernolle, and P. Pribyl, Geophys. Res. Lett. **41**, 7413, doi:10.1002/2014GL061820 (2014).
[19]L. Romagnani, S. V. Bulanov, M. Borghesi, P. Audebert, J. C. Gauthier, K. Löwenbrück, A. J. Mackinnon, P. Patel, G. Pretzler, T. Toncian, and O. Willi, Phys. Rev. Lett. **101**, 025004 (2008).
[20]Y. Kuramitsu, Y. Sakawa, T. Morita, C. D. Gregory, J. N. Waugh, S. Dono, H. Aoki, H. Tanji, M. Koenig, N. Woolsey, and H. Takabe, Phys. Rev. Lett. **106**, 175002 (2011).
[21]J. S. Ross, H.-S. Park, R. Berger, L. Divol, N. L. Kugland, W. Rozmus, D. Ryutov, and S. H. Glenzer, Phys. Rev. Lett. **110**, 145005 (2013).
[22]R. Presura, S. Neff, and L. Wanex, Astrophys. Space Sci. **307**, 93 (2007).
[23]R. P. Drake, Phys. Plasmas **7**, 4690 (2000).
[24]Y. P. Zakharov, IEEE Trans. Plasma Sci. **31**, 1243 (2003).
[25]W. Gekelman, H. Pfister, Z. Lucky, J. Bamber, D. Leneman, and J. Maggs, Rev. Sci. Instrum. **62**, 2875 (1991).
[26]C. Niemann, C. G. Constantin, D. B. Schaeffer, A. Tauschwitz, T. Weiland, Z. Lucky, W. Gekelman, E. T. Everson, and D. Winske, J. Instrum. **7**, P03010 (2012).
[27]G. Dimonte and L. G. Wiley, Phys. Rev. Lett. **67**, 1755 (1991).
[28]A. Collette and W. Gekelman, Phys. Rev. Lett. **105**, 195003 (2010).
[29]D. B. Schaeffer, E. T. Everson, A. S. Bondarenko, S. E. Clark, C. G. Constantin, S. Vincena, B. V. Compernolle, S. K. P. Tripathi, D. Winske, W. Gekelman, and C. Niemann, Phys. Plasmas **21**, 056312 (2014).
[30]D. B. Schaeffer, E. T. Everson, D. Winske, C. G. Constantin, A. S. Bondarenko, L. A. Morton, K. A. Flippo, D. S. Montgomery, S. A. Gaillard, and C. Niemann, Phys. Plasmas **19**, 070702 (2012).
[31]S. H. Batha, R. Aragonez, F. L. Archuleta, T. N. Archuleta, J. F. Benage, J. A. Cobble, J. S. Cowan, V. E. Fatherley, K. A. Flippo, D. C. Gautier, R. P. Gonzales, S. R. Greenfield, B. M. Hegelich, T. R. Hurry, R. P. Johnson, J. L. Kline, S. A. Letzring, E. N. Loomis, F. E. Lopez, S. N. Luo, D. S. Montgomery, J. A. Oertel, D. L. Paisley, S. M. Reid, P. G. Sanchez, A. Seifter, T. Shimada, and J. B. Workman, Rev. Sci. Instrum. **79**, 10F305 (2008).
[32]D. W. Hewett, S. H. Brecht, and D. J. Larson, J. Geophys. Res. **116**, 12, doi:10.1029/2011JA016904 (2011).
[33]S. E. Clark, D. Winske, D. B. Schaeffer, E. T. Everson, A. S. Bondarenko, C. G. Constantin, and C. Niemann, Phys. Plasmas **20**, 082129 (2013).
[34]V. P. Bashurin, A. I. Golubev, and V. A. Terekhin, J. Appl. Mech. Tech. Phys. **24**, 614 (1983).
[35]A. I. Golubev, A. A. Solov'ev, and V. A. Terekhin, J. Appl. Mech. Tech. Phys. **19**, 602 (1979).
[36]D. J. Larson, D. Winske, M. M. Cowee, S. E. Clark, C. Niemann, and S. H. Brecht, J. Radiat. Eff. Res. Eng. **34**, 1–10 (2016).
[37]D. B. Schaeffer, A. S. Bondarenko, E. T. Everson, S. E. Clark, C. G. Constantin, and C. Niemann, J. Appl. Phys. **120**, 043301 (2016).